J. Serb. Chem. Soc. 70 (6) 879– 889 (2005)
JSCS – 3323

UDC 669.1'28:66.087:66.097
Original scientific paper

Electrodeposition and characterization of Fe–Mo alloys as cathodes for hydrogen evolution in the process of chlorate production

N. ELEZOVIĆ[1,#] , B. N. GRGUR[2,*,#], N. V. KRSTAJIĆ[2] and V. D. JOVIĆ[1,#]

[1]*Center for Multidisciplinary Studies, University of Belgrade, P. O. Box 33, 11030 Belgrade and* [2]*Faculty of Technology and Metallurgy, University of Belgrade, Karnegijeva 4, 11000 Belgrade, Serbia and Montenegro (e-mail: BNGrgur@tmf.bg.ac.yu)*

(Received 20 July, revised 20 October 2004)

Abstract: Fe–Mo alloys were electrodeposited from a pyrophosphate bath using a single diode rectified AC current. Their composition and morphology were investigated by SEM, optical microscopy and EDS, in order to determine the influence of the deposition conditions on the morphology and composition of these alloys. It was shown that the electrodeposition parameters, such as: chemical bath composition and current density, influenced both the composition of the Fe–Mo alloys and the current efficiency for their deposition, while the micro and macro-morphology did not change significantly with changing conditions of alloy electrodeposition. It was found that the electrodeposited Fe–Mo alloys possessed a 0.15 V to 0.30 V lower overvoltage than mild steel for hydrogen evolution in an electrolyte commonly used in commercial chlorate production, depending on the alloy composition, *i.e.*, the conditions of alloy electrodeposition.

Keywords: Fe–Mo alloy, electrodeposition, morphology, catalitic activity.

INTRODUCTION

Binary and ternary alloys containing transition metals, such as Mo,W, Ni, Co and Fe, electrodeposited under direct current (DC) conditions have been described in the literature as promising cathodes for hydrogen evolution in chlor–alkaline and chlorate electrolysis.[1–4] It was shown that certain deposit compositions tend to lower the hydrogen evolution overvoltage and it is anticipated that these new cathodic materials may perform better than those used commercially in industrial plants.[4]

The influence of pulse plating on the current efficiency, composition and deposit morphology has also been examined.[5] Asquare wave pulsing regime was used to produce Co–Mo alloy coatings containing up to 55 at.%molybdenum. Due to the co-generation of hydrogen at these deposition potentials, deposit current efficiencies of about

Serbian Chemical Society active member.
* Author correspondence.

50 % are typical. Deposits of poor quality were obtained using deposition current densities higher than 150 mA cm^{-2}, while micor-cracked, compact coatings were obtained at current densities of 25 mA cm^{-2} to 150 mA cm^{-2}. The polarization characteristics of coatings deposited at high frequency (10^4 Hz) using an effective current density of 25 mA cm^{-2} have been investigated in electrolytes commonly used in brine electrolysis. It was shown that the overvoltage for hydrogen evolution on the Co–Mo alloy was about 0.15 V lower than that observed on mild steel.[6]

During the last decade, numerous papers concerning the mechanism and kinetics of induced co-deposition, particularly for the systems Ni–Mo and Ni–W, were published,[7–14] but none of these works was devoted to the influence of the deposition conditions on the morphology of the electrodeposited alloys and the influence of their composition on the hydrogen evolution reaction.

In this paper, the morphology and composition of Fe–Mo alloy thin films were examined for a variety of electrodeposition conditions and their influence on the hydrogen evolution reaction in a commercial electrolyte for chlorate electrolysis was investigated.

EXPERIMENTAL

All samples were deposited on mild steel substrates having a surface area of 3 cm^2. The steel substrates were first sand blasted using 50 μm particles, degreased in NaOH-saturated ethanol for min, then etched in 25 wt. % HCl for 2 min. After this procedure, the samples were washed with distilled water, dried and weighed and then immersed in the solution for Fe–Mo alloy electrodeposition. After deposition, the samples were washed, dried and weighed again to determine the mass of the alloy. All solutions were made using distilled–deionized water and analytical grade chemicals.

Fe–Mo alloys were deposited to a constant charge of 36 C cm^{-2}, in two electrode plating bath from solutions containign different concentrations of $FeCl_3$ and $Na_4P_2O_7$ with constant concentrations of $NaHCO_3$ (75 g dm^{-3}) and Na_2MoO_4 (40 g dm^{-3}) at 60 ºC. A Ti–Pt mesh, placed parallel to the cathode, was used as a counter electrode during electrodeposition and the electrolyte was moderately stirred with a magnetic stirrer.

All deposition experiments were performed using a home made single diode rectifier. A potentiostat PAR M273 was used to collect the current–voltage data for hydrogen evolution. These polarization curves were corrected for IR drop after determining the solution resistance from the high frequency intercept on the Z' axis of Z'– Z" impedance plots. Impedance diagrams were performed using a potentiostat PAR M273 and a Lock-in Amplifier PAR M5301 with software for impedance measurements PAR M378.

The hydrogen evolution on the Fe–Mo electrodeposits was investigated in a standard electrochemical cell using electrolyte for chlorate production, 300 g dm^{-3} NaCl and 3 g cm^{-3} $K_2Cr_2O_7$ at 80 ºC. A saturated calomel electrode (SCE) was used as the reference electrode while a flat Pt sheet served as the counter electrode.

Scanning electron microscopy (SEM – JOEL 840) was used to characterize the as-deposited surfaces and to determine the alloy composition using energy dispersive X-ray spectroscopy (EDS). Selected deposits were mounted in cross-section, polished and examined by optical microscopy.

RESULTS

Fe–Mo alloy electrodeposition

In order to determine the optimum conditions for Fe–Mo alloy electrodeposition, the concentration of $FeCl_3$ was varied between 3 and 12 g dm^{-3}, the concentration of $Na_4P_2O_7$ was varied between 15 and 75 g dm^{-3} and the current density between 10

and 100 mA cm^{-2}. After determining the composition of the Fe–Mo alloys by EDS analysis, the current efficiency (η_j) was calculated using the expression given by Lowenheim:[15]

$$\eta_j = \frac{\Delta m}{m_t} = \frac{\Delta m(x_{Mo}\varepsilon_{Fe} + x_{Fe}\varepsilon_{Mo})}{I\tau\varepsilon_{Mo}\varepsilon_{Fe}} \quad (1)$$

where: Δm – mass of deposited alloy; m_t – theoretical mass; x_{Mo} – wt.% of Mo in the deposit; x_{Fe} – wt.% of Fe in the deposit; ε_{Fe} and ε_{Mo} – electrochemical equivalents of Fe and Mo, respectively; I – current; t – duration of the deposition process.

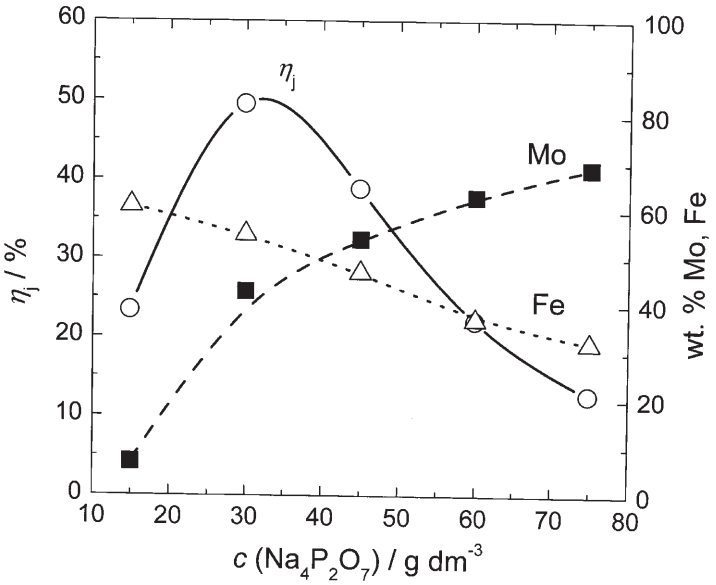

Fig. 1. The influence of the $Na_4P_2O_7$ concentration on the current efficiency (η_j) and alloy composition (wt.% Mo, Fe) recorded at an average current density of a rectified AC current regime of 20 mA cm^{-2}: composition of the electrolyte – 9 g dm^{-3} $FeCl_3$, 75 g dm^{-3} $NaHCO_3$ and 40 g dm^{-3} Na_2MoO_4; temperature – 60 ºC.

The influence of the $Na_4P_2O_7$ concentration. The influence of the $Na_4P_2O_7$ concentration on the current efficiency and alloy composition was investigated in a solution containing 9 g dm^{-3} $FeCl_3$, 75 g cm^{-3} $NaHCO_3$ and 40 g dm^{-3} Na_2MoO_4 at an average current density of 20 mA cm^{-2}. As can be seen from Fig. 1, the content of Mo increases while the content of Fe decreases with increasing concentation of $Na_4P_2O_7$. The current efficiency is seen to possess a maximum of about 50 % at a concentration of $Na_4P_2O_7$ of 30 g dm^{-3}.

The influence of the $FeCl_3$ concentration. The influence of the $FeCl_3$ concentration on the current efficiency and alloy composition was investigated in a solution containing 45 g dm^{-3} $Na_4P_2O_7$, 75 g dm^{-3} $NaHCO_3$ and 40 g dm^{-3} Na_2MoO_4 at an average current density of 20 mA cm^{-2}. As can be seen in Fig. 2, the content of Mo decreases, while the content of Fe increases with increasing concentration of $FeCl_3$. The current efficiency also incrases with increasing concentration of $FeCl_3$.

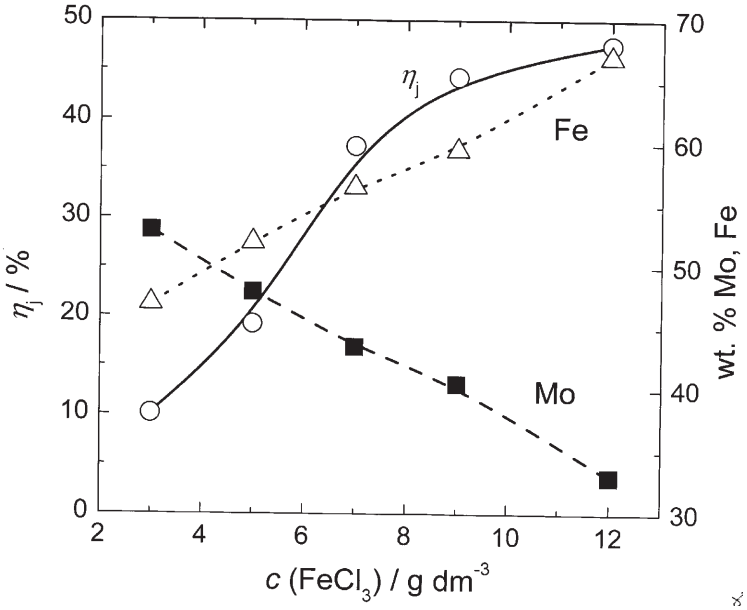

Fig. 2. The influence of the $FeCl_3$ concentration on the current efficiency (η_j) and alloy composition (wt.% Mo, Fe) recorded at an average current density of a rectified AC current regime of 20 mA cm^{-2}: composition of the electrolyte – 45 g dm^{-3} $Na_4P_2O_7$, 75 g dm^{-3} $NaHCO_3$ and 40 g dm^{-3} Na_2MoO_4; temperature – 60 ºC.

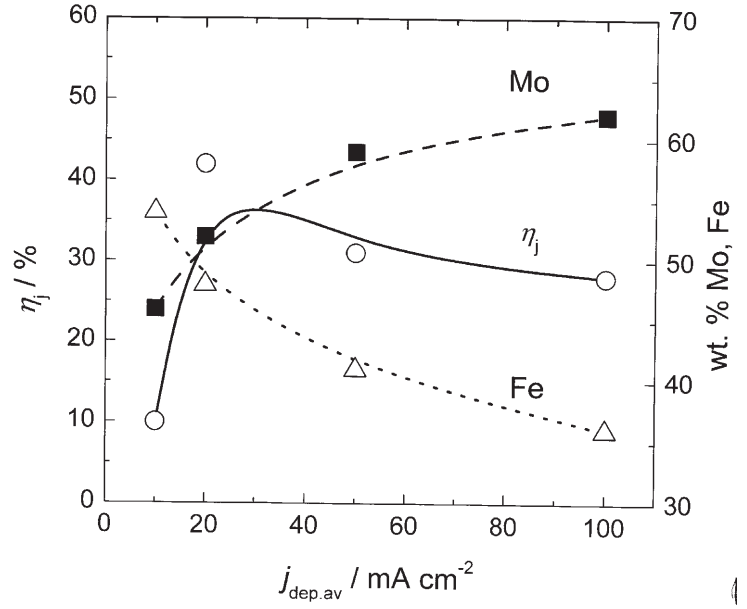

Fig. 3. The influence of the average current density for alloy deposition ($j_{dep.av}$) on the current efficiency (η_j) and alloy composition (wt.% Mo, Fe) recorded in an electrolyte containing 45 g dm^{-3} $Na_4P_2O_7$, – 9 g dm^{-3} $FeCl_3$, 75 g dm^{-3} $NaHCO_3$ and 40 g dm^{-3} Na_2MoO_4 at a temperature of 60 ºC.

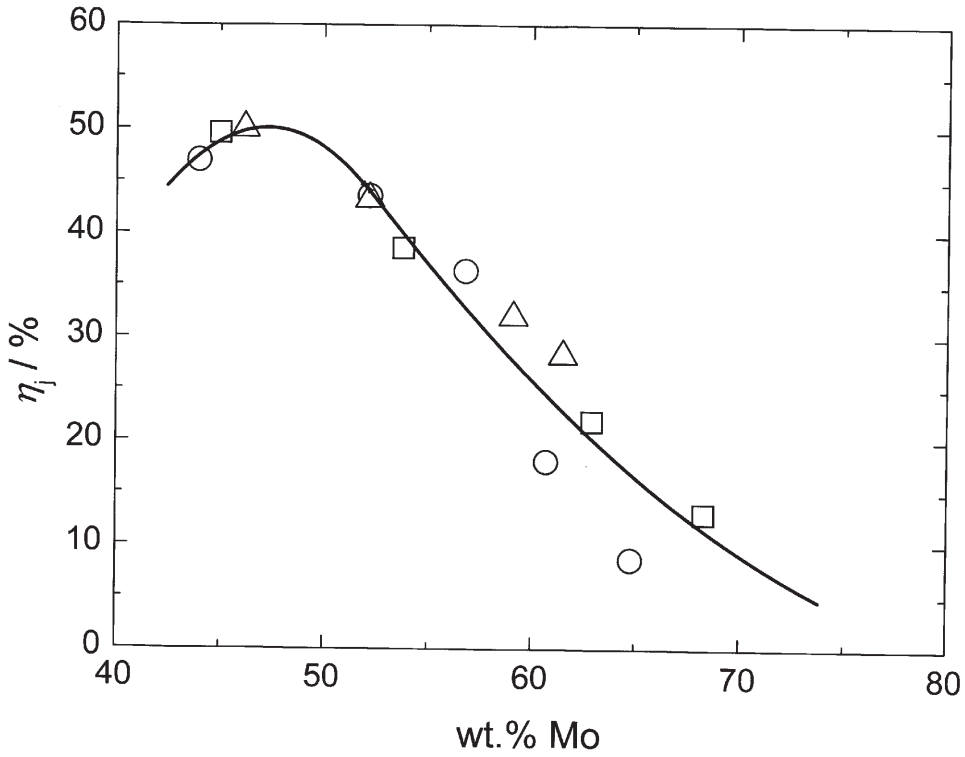

Fig. 4. Dependence of η_j on the alloy composition (wt.% Mo): (□) the influence of the $Na_4P_2O_7$ concentration; (○) the influence of the $FeCl_3$ concentration; (Δ) the influence of the average current density for alloy deposition.

The influence of the average current density. The influence of the average current density on the current efficiency and alloy composition was investigated in a solution containing 9 g cm^{-3} $FeCl_3$, 45 g dm^{-3} $Na_4P_2O_7$, 75 g dm^{-3} $NaHCO_3$ and 40 g dm^{-3} Na_2MoO_4 and the results are shown in Fig. 3. As can be seen, the content of Mo increases, while the content of Fe decreases with increasing average current density, while the current efficiency increases sharply from 10 % to 43 % in the range between 10 mA cm^{-2} and 20 mA cm^{-2}, reaching a maximum of 43 % at 20 mA cm^{-2}, and then slowly decreases to about 30 % with increasing average current density from 20 mA cm^{-2} to 100 mA cm^{-2}.

Summarizing all the results presented in Figs. 1, 2 and 3, the current efficiency can be plotted as a function of the composition of the Fe–Me alloy, as is shown in Fig. 4. The maximum current efficiency of about 50 % was obtained at a content of Mo of about 47 wt.%.

Morphology of the Fe–Me alloys

The morphology of the as-deposited samples was investigated by SEM of the electrode surface and optical microscopy of a cross section. In Fig. 5 are shown a typical top view of an Fe–Mo alloy (a) and a cross section of a deposit of thickness of about

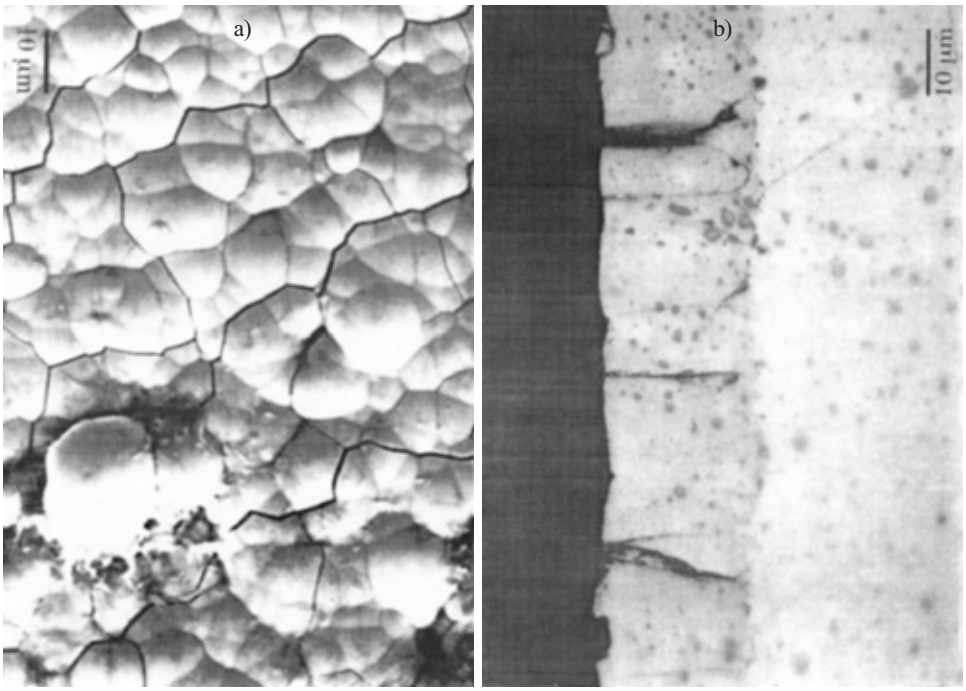

Fig. 5. (a) Typical SEM top view of an Fe–Mo alloy; (b) Typical cross-section of an about 20 μm thick Fe–Mo alloy deposit.

20 μm (b). As can be seen, the morphology of the Fe–Mo alloys is characterized by the presence of micro-cracks, with some of them being up to 2 μm wide (Fig. 5b). It is important to note that although the surface of the samples deposited at lower current densities (examined with the naked eye) appeared to be less rough, *i.e.*, brighter, SEM showed that the micro-morphology of all the samples was almost the same.

Polarization diagrams in the electrolyte for chlorate production

Polarization curves for mild steel (□) and one of the alloys with a lower overvoltage for hydrogen evolution (○), recorded in a commercial solution for chlorate production (300 g dm^{-3} NaCl and 3 g dm^{-3} $K_2Cr_2O_7$) at 80 ºC are shown in Fig. 6. As can be seen, constant Tafel slopes of 190 – 200 mV dec^{-1} were obtained.

Finally, all samples were tested under the same condition for the hydrogen evolution reaction. The results are summarized in Fig. 7, where the electrode potentials recorded at a current density of 200 mA cm^{-2} are plotted as a function of Mo content in the alloy. As can be seen, the lowest overpotential was recorded for samples containing about 60 wt.% Mo.

If the sample is left in the cell for hydrogen evolution at a current density of 200 mA cm^{-2} for a longer time (up to 120 h), the polarization characteristics change, as can be seen in Fig. 8, most probably as a consequence of a small change of the surface roughness during extended hydrogen evolution at the investigated surface.

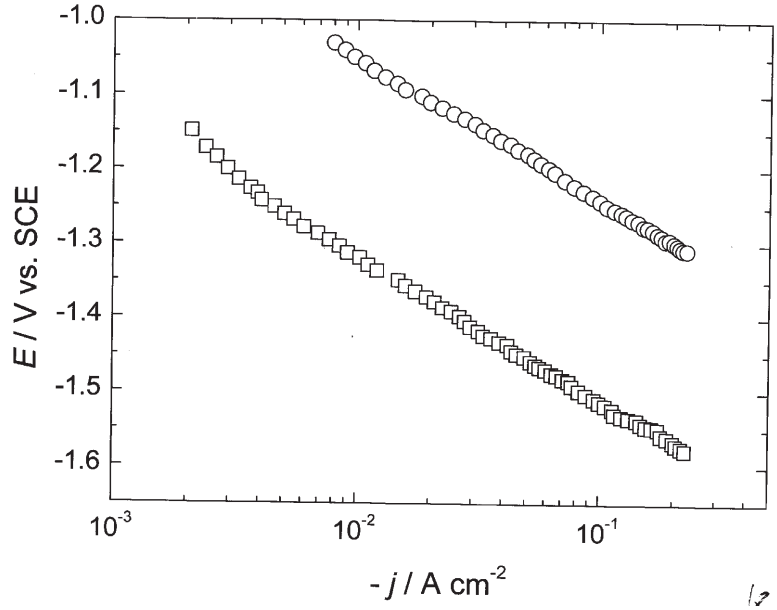

Fig. 6. Polarization characteristics for mild steel (□ and Fe–Mo alloy containing 61.5 wt.% Mo (○) recorded in a commercial electrolyte for chlorate production: 300 g dm^{-3} NaCl, 3 g dm^{-3} $K_2Cr_2O_7$ at 80 ºC.

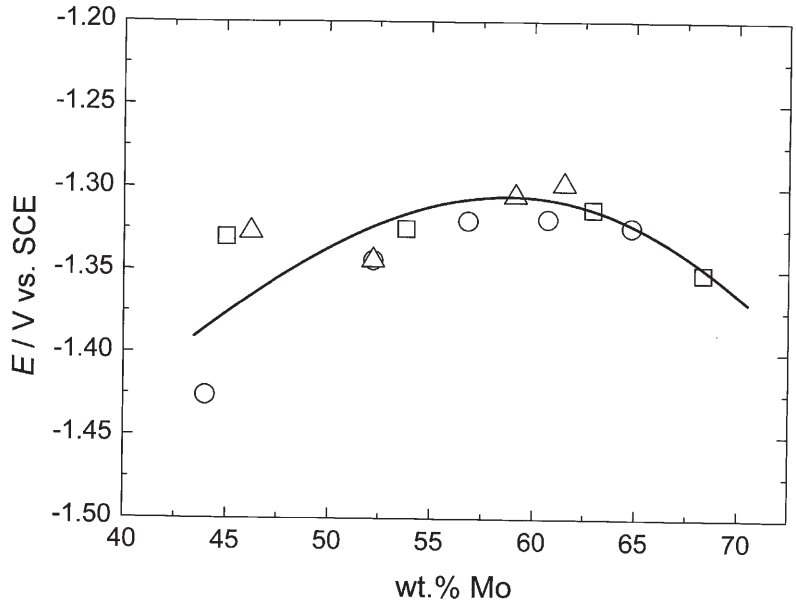

Fig. 7. Dependence of the hydrogen evolution potential for different Fe–Mo alloys recorded at a current density of 200 mA cm^{-2}. Electrolyte: 300 g dm^{-3} NaCl, 3 g dm^{-3} $K_2Cr_2O_7$ at 80 ºC. (□) Samples obtained by changing the $Na_4P_2O_7$ concentration; (○) samples obtained by changing the $FeCl_3$ concentration; (Δ) samples obtained by changing the average current density for alloy deposition.

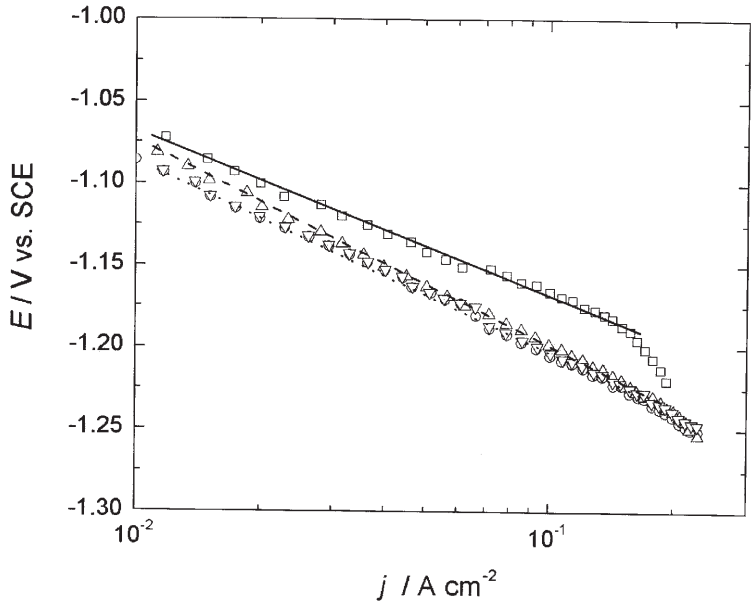

Fig. 8. Polarization characteristics of an about 20 μm thick Fe–Mo alloy deposit containing about 55 wt.% Mo recorded under the same conditions as in Fig. 6. (○) Polarization characteristics recorded immediately after immersion in the electrolyte, Tafel slope –128 mV dec^{-1} (dash-dot line); (▽) after 24 h of hydrogen evolution at 200 mA cm^{-2}, Tafel slope –128 mV dec^{-1} (dash-dot line); (△) after 48 h of hydrogen evolution at 200 mA cm^{-2}, Tafel slope –123 mV dec^{-1} (dashed line); (□) after 120 h of hydrogen evolution at 200 mA cm^{-2}, Tafel slope –97 mV dec^{-1} (full line).

DISCUSSION

The influence of the electrodeposition conditions on the composition and morphology of Fe–Mo alloys

After examining the results presented in Figs. 1 and 2, obtained at an average current density of 20 mA cm^{-2}, it was concluded that the influence of the average current density should be investigated in a solution containing 9 g dm^{-3} $FeCl_3$ and 45 g dm^{-3} $Na_4P_2O_7$, since with this solution, the content of Mo in the alloy was high, between 40 wt.% and 50 wt.%, while the current efficiency for alloy deposition was about 40 %, slightly lower than the maximum of 50 % recorded with a concentration of $Na_4P_2O_7$ of 30 g dm^{-3}.

As can be seen in Fig. 3, an average current density lower than 20 mA cm^{-2} is not recommendable, since the current efficiency (η_j) is only 10 % and the content of Mo is also low, about 25 wt.%. At average current densities higher than 20 mA cm^{-2}, η_j slightly decreases, while the content of Mo increases to about 62 wt.% at j = 100 mA cm^{-2}.

If all results presented in Figs. 1–3 are summarized, Fig. 4 is obtained. Hence, a maximum η_j for Fe–Mo alloy electrodeposition of 50 % could be obtained at Mo content in the alloy of about 47 wt.%. At higher contents of Mo in the alloy, η_j decreases

down to about 15 % at 68 wt.% of Mo. As was to be expected, the decrease of η_j is the consequence of the increase of the content of Mo in the electrodeposited alloy.

The influence of alloy composition on the overvoltage for hydrogen evolution in a commercial electrolyte for chlorate production

Well defined Tafel lines with a single slope varying between 190 mV dec^{-1} and 250 mV dec^{-1} were obtained for all the investigated samples (polarization curves in a commercial electrolyte for each electrodeposited sample). The unusually high values of the Tafel slope, also obtained for mild steel (as seen in Fig. 6), cannot be explained using formal electrochemical kinetics. Such a behavior is most probably the consequence of the presence of dichromate (added to the electrolyte to prevent cathodic losses, *i.e.*, reduction of hypochlorite). It is known[16,17] that under such conditions a semi-permeable chromium polyoxide film forms on the cathode surface, causing an additional potential drop and, consequently, a higher value of the Tafel slope.

All the results for the hydrogen evolution reaction are summarized in Fig. 7. It can be concluded that the lowest overvoltage for hydrogen evolution at a current density of 200 mA cm^{-2} (usually used in industrial plants) is obtained with Fe–Mo alloys containing about 60 wt.% of Mo in the alloy. Considering the phase diagram of the Fe–Mo alloy,[18] it can be seen that in this region of alloy composition, the intermetallic compound $FeMo_3$ is predominant. According to Jakšić *et. al.*,[19,20] the exchange current density for hydrogen evolution can be up to two orders of magnitude different for different intermetallic compounds. Hence, it seems reasonable to expect that the highest catalytic activity for hydrogen evolution would be obtained with alloys in which the $FeMo_3$ intermetallic compound should be predominant. An attempt was made to examine the as-deposited, 20 μm thick layer of a Fe–Mo alloy of such a composition by the X-ray technique, in order to identify some of the possible intermetallic compounds. Unfortunately, because of the very small size of the crystallites, lower than the limit of the technique, this attempt was unsuccessful.

Taking into account the morphology of the electrodeposited samples, *i.e*, the presence of open pores of up to 2 μm wide (Fig. 5b), it is not surprising that the polarizaiton characteristic of the deposit changes with the exposure time of such surface to hydrogen evolugion (Fig. 8). Such a behavior is most probably caused by an increase of the real surface area after prolonged hydrogen evolution, which lowers the real current density and, accordingly, overvoltage for hydrogen evolution.

Finally, the main purpose of all the investigations performed in this work was to show that electrodeposited Fe–Mo alloys could be used as cathodes for chlorate production. This is confirmed by the results of a pilot plant test lasting for 244 days, in which one of the samples (among several samples tested, showing similar results) of approximate the content of 50 wt.% and a thickness of about 20 μm was tested. The cell voltage was about 0.3 V lower than that with a commercial mild steel cathode (the results are not presented in this article), indicating that Fe–Mo alloys could be successfully used as a catalytically active cathode in an industrial plant for the production of chlorate.

CONCLUSION

It has been shown that the electrodeposition parameters (concentration of $Na_4P_2O_7$ and $FeCl_3$ salts and average current density of deposition) influence both the composition of the Fe–Mo alloys and the current efficiency for their deposition, while the micro and macro-morphology did not change significantly with changing conditions of alloy electrodeposition.

Further, it has been shown that the electrodeposited Fe–Mo alloys possess an about 0.15V to about 0.30V lower overvoltage than mild steel for hydrogen evolution in an electrolyte commonly used in commercial chlorate production, depending on the alloy composition, indicating that Fe–Mo alloys could be used as catalytically active cathodes for the production of chlorate in industrial plants.

Acknowledgement: The authors are indebted to theMinistry of Science and Technology of the Republic of Serbia for the financial support of this work, under the project number 101825.

И З В О Д

ЕЛЕКТРОХЕМИЈСКО ТАЛОЖЕЊЕ И КАРАКТЕРИЗАЦИЈА Fe-Mo ЛЕГУРА КАО КАТОДА ЗА РЕАКЦИЈУ ИЗДВАЈАЊА ВОДОНИКА У ИНДУСТРИЈСКОМ ПРОЦЕСУ ПРОИЗВОДЊЕ ХЛОРАТА

Н. ЕЛЕЗОВИЋ[1], Б. Н. ГРГУР[2], Н. В. КРСТАЈИЋ[2], В. Д. ЈОВИЋ[1]

[1]*Центар за мултидисциплинарне студије Универзитета у Београду, п. Пр. 33, 11030 Београд и*
[2]*Технолошко-металуршки факултет Универзитета у Београду, Карнегијева 4, 11000 Београд*

Fe–Mo легуре су електрохемијски таложене из пирофосфатног купатила коришћењем периодично промењивог AC струјног режима. Састав и морфологија добијених талога испитивани су SEM и EDS техникама, док је попречни пресек узорака испитиван оптичком микроскопијом, са циљем да се одреди утицај услова таложења на морфологију и састав легура. Показано је да услови таложења, састав купатила и густина струје таложења, практично не утичу на морфологију легура, али да утичу на састав легура и на искоришћење струје њиховог таложења. Такође је показано да исталожене легуре поседују мању пренапетост за реакцију издвајања водоника од меког челика (0.15 Vдо 0.30 V у зависности од услова таложења) који се користи као катода у индустријским постројењима за производњу хлората, указујући да се елекктрохемијски исталожене Fe-Mo легуре могу користити као каталитички активне катоде у овом процесу.

(Примљено 20. јула, ревидирано 20. октобра 2004.)

REFERENCES

1. H. S. Myers, *PhD Thesis*, Columbia University, 1961
2. L. O. Case, A. Korhn, *J. Electrochem. Soc.* **105** (1958) 512
3. A. Krohn, T. Brown, *J. Electrochem. Soc.* **108** (1961) 60
4. J. R. Hall, J. T. Van Gemert, *U. S. Patent* 3,291,714 (1966)
5. N. Krstajić, K. Popov, M. Spasojević, R. Atanasoski, *J. Appl. Electrochem.* **12** (1982) 435
6.M. Spasojević, N. Krstajić, P. Despotov, R. Atanasoski, *J. Appl. Electrochem.* **14** (1983) 265

7. E. J. Podlaha, D. Landolt, *J. Electrochem. Soc.* **143** (1996) 885
8. D. Landolt, *Electrochim. Acta* **39** (1994) 1075
9. E. J. Podlaha, D. Landolt, *J. Electrochem. Soc.* **143** (1996) 893
10. E. J. Podlaha, D. Landolt, *J. Electrochem. Soc.* **144** (1997) 1672
11. T. A. Alekhina, I. A. Shoshina, B. M. Korbassov, *Electrochimiya* **30** (1994) 269
12. R. S. Lillard, G. S. Kanner, D. P. Butt, *J. Electrochem. Soc.* **145** (1998) 2718
13. O. Younes, E. Gileadi, *Electrochem. Solid State Lett.* **3** (2000) 543
14. O. Younes, E. Gileadi, *J. Electrochem. Soc.* **149** (2002) C100-C111
15. F. A. Lowenhiem, *Modern Electroplating*, 3rd Edition (Editor), Wiley, New York, 1974
16. E. Muller, *Z. Elektrochem.* **6** (1899) 469
17. T. Nagai, T. Takei, *J. Electrochem. Soc. Japan* **25** (1957) 373
18. M. Hansen, K. Andrenko, *Constitution of Binary Alloys*, Mc-Graw Hill, New York, 1958
19. M. M. Jakšić, *J. Mol. Catal.* **38** (1986) 161
20. M. M. Jakšić, *Mat. Chem. Phys.* **22** (1989) 1.